

Resonance-channel quantum numbers in electron-hydrogen and proton-hydrogen scattering from group theory of the long-range dipole interaction

David R. Herrick*

Bell Laboratories, Murray Hill, New Jersey 07974

(Received 18 March 1975)

We derive quantum numbers K and T which label asymptotic potential-energy curves in e^- -H scattering. Zero-order channel states are constructed group theoretically so that the dipole interaction $r_1 \cos \theta_{12}$ is diagonal in a product space of hydrogenic orbitals for 1 and spherical harmonics for 2. K and T are analogous to the "electric quantum number" and the z component of angular momentum in the linear Stark effect for H, and are closely related to quantum numbers described recently for doubly excited He. Channels supporting resonances are predicted from a perturbation expansion of eigenvalues of the effective centrifugal barrier operator $2r_1 \cos \theta_{12} + l^2/2$ in terms of K and T . Comparison with exact H^- results and experiment is excellent, and the method accounts for previously unexplained degeneracies with respect to total parity. A rigorous result is that only channels with $K > 0$ can support an infinity of states below threshold. An approximate selection rule for coupling between neighboring channels suggests that decay of H^- resonances goes preferentially to channels such that $\Delta K = \pm 1$, $\Delta T = 0$. Application of the method is also made to p -H scattering channels for which the zero-order basis nearly diagonalizes the long-range centrifugal barrier.

I. INTRODUCTION

In this paper we analyze group theoretically the long-range dipole classification of resonance channels in electron-hydrogen compound states. New channel quantum numbers are derived which lead to predictions of channels supporting either resonances below threshold or shape resonances. The quantum numbers are similar to those offered earlier¹⁻³ to classify mixings of degenerate hydrogenic configurations² and to classify energy levels and autoionization widths of Rydberg series of doubly excited states.³ The present results explain in detail the empirical systematics of the H^- spectrum noted in the previous work. The group-theoretic significance of the present theory is that at the outset we attempt to classify resonance channels rather than the individual resonances themselves.

The physical characterization of the H^- resonance channels to which we apply the group theory is the long-range dipole approximation.^{4,5} This method has been in use for some time to interpret resonances in both electron-hydrogen impact excitation⁴⁻⁶ and photoionization⁷ cross sections. These earlier results were treated in an empirical fashion, although as we now show the problem is actually quite rich in both physical and group-theoretic content.

The format of the paper is as follows. A general statement of the problem and the approximations involved appears in Sec. II. The group theory necessary to describe the channels is offered in Sec. III, followed by the actual derivation and a physical interpretation of the new channel quantum numbers in Sec. IV. We show also in this section

that there is an interesting analogy between the present classification and the $SU(3)$ symmetry⁸ of strongly interacting particles. Results of our method, including a perturbation expansion of the channel interactions, predictions of degeneracies and shape resonances, and comparison with experiment and other theory, appear in Sec. V.

In Sec. VI we apply the channel quantum numbers to the related problems of positron-hydrogen and proton-hydrogen resonances. In the latter case the group-theoretic classification of channels described herein is in fact a classification of the adiabatic molecular H_2^+ potential-energy curves in the region of large internuclear separation. Inclusion of the molecular centrifugal barrier as a small perturbation then provides a concise description of the dynamical H_2^+ states.

II. STATEMENT OF PROBLEM

We outline in this section a method of describing the asymptotic regime of doubly excited two-electron atoms which allows (Sec. III) a group-theoretical characterization of the resonance channels. The Hamiltonian is

$$H = -\frac{1}{2}(\nabla_1^2 + \nabla_2^2) - \frac{1}{r_1} - \frac{1}{r_2} + \frac{\lambda}{r_{12}}, \quad (1)$$

with values of the coupling parameter $\lambda = 1, \frac{1}{2}, \frac{1}{3}, \dots$ corresponding in this system of units to the isoelectronic series H^-, He, Li^+, \dots . At $\lambda = 0$ the energy is hydrogenic:

$$E(\lambda = 0) = -\frac{1}{2}(N^2 + n^2),$$

where $N (= 1, 2, \dots)$ labels the ionization threshold and $n (= N + 1, N + 2, \dots)$ labels the Rydberg series

of states below the N th threshold. When $\lambda > 0$ the doubly excited spectrum (i.e., $N \geq 2$) is no longer discrete, owing to interaction of the zero-order bound states with continuum channels of lower thresholds, and the states correspond to physically observable resonances.⁹ Neglecting exchange, the wave functions for total orbital angular momentum L and parity π can be expanded for $r_2 > r_1$ as

$$|\Psi\rangle = \sum_{N, l, l'} |Nl, l'; LM\pi\rangle F(l, l', r_2), \quad (2)$$

where $|Nl, l'; LM\pi\rangle$ is a five-coordinate *channel state* representing the radial and angular coordinates of electron 1 and the angular coordinates of electron 2, with

$$|Nl, l'; LM\pi\rangle = \sum_{m, m'} |Nlm\rangle_1 |l'm'\rangle_2 \langle lm, l'm' | LM \rangle. \quad (3)$$

Here $|Nlm\rangle$ is a hydrogenic target state and $\langle lm, l'm' | LM \rangle$ is the $SO(3)$ Clebsch-Gordan coefficient. We use the Condon-Shortley phase convention¹⁰ for spherical harmonics, and the radial functions are taken to behave as $(-r)^l$ near the origin. The expansion coefficients in Eq. (2) are radial functions for electron 2. In what follows we use a closed-channel close-coupling approximation¹¹ to states below the N th threshold, in which a truncated wave function $|\Psi_N\rangle$ is obtained by keeping only terms of constant N in the eigenfunction expansion Eq. (2). Thus coupling to continuum channels of lower thresholds is ignored, so that resonance channels are represented as bound states.

Use of the *configuration channel basis*, $|Nl, l'; L\pi\rangle$, as a starting point is arbitrary. If we define an orthogonal transformation of channel states with new quantum numbers denoted collectively by the label d ,

$$|Nl, l'; L\pi\rangle = \sum_d |Nd; L\pi\rangle U(d, l, l'), \quad (4)$$

then there is an induced transformation on the radial coefficients:

$$|\Psi_N\rangle = \sum_d |Nd; L\pi\rangle F(d, r_2), \quad (5a)$$

$$F(d, r_2) = \sum_{l, l'} U(d, l, l') F(l, l', r_2). \quad (5b)$$

Using $\langle NdL\pi | H - E | \Psi_N \rangle = 0$, one obtains the coupled radial equation

$$\left(\frac{d^2}{dr_2^2} + \frac{2}{r_2} \frac{d}{dr_2} + k^2 \right) F(d, r_2) = \sum_{d'} V_{dd'}(r_2) F(d', r_2), \quad (6)$$

where in the present approximation of fixed N

$$V_{dd'}(r_2) = \langle NdL\pi | \left(\frac{\hat{p}_2^2}{r_2^2} + \frac{2\lambda}{r_{12}} - \frac{2}{r_2} \right) | Nd'L\pi \rangle. \quad (7)$$

A group-theoretic classification of the resonance channels in this approximation thus amounts to finding the channel basis which minimizes the off-diagonal $V_{dd'}$, and in the event of an exact symmetry gives $V_{dd'} = 0$ when $d' \neq d$. This problem is somewhat simpler than that of characterizing the exact wave functions, since only the hydrogenic radial functions of electron 1 are involved.

Following Seaton,⁴ for large r_2 the coupling terms to order r_2^{-2} are

$$V_{dd} = 2(\lambda - 1)r_2^{-1} + \langle NdL\pi | \hat{A} | NdL\pi \rangle r_2^{-2}, \quad (8)$$

$$V_{dd'} = \langle NdL\pi | \hat{A} | Nd'L\pi \rangle r_2^{-2} \quad (d \neq d'). \quad (9)$$

Here $\hat{A} = \hat{A}_0 + \hat{A}_1$, with

$$\hat{A}_0 = 2\lambda r_1 \cos\theta_{12}, \quad \hat{A}_1 = \hat{p}_2^2. \quad (10)$$

The *dipole representation*^{6(b)} of the channel states is that basis in which the matrix ($=A$) of \hat{A} is diagonal. Then for large r_2 ($\equiv r$) Eq. (6) is uncoupled to order r^{-2} ,

$$\left(\frac{d^2}{dr^2} + \frac{2}{r} \frac{d}{dr} + k^2 - \frac{2(\lambda - 1)}{r} - \frac{a_j}{r^2} \right) F_j(d, r) = 0, \quad (11)$$

where a_j is the eigenvalue of A for the j th channel state in the dipole basis. When $\lambda < 1$ there are an infinite number of bound-state radial solutions in each channel j , owing to the long-range attractive Coulomb potential. Gailitis and Damburg,⁵ using the analysis of the r^{-2} potential by Landau and Lifshitz,¹² noted that for H^- (i.e., $\lambda = 1$) only resonance channels in which $a_j < -\frac{1}{4}$ could support asymptotically an infinite number of states—and thus correspond to observable resonances below threshold. This criterion follows also from the fact that solutions to Eq. (11) are bases for irreducible representations of an $SO(2, 1)$ -type radial algebra.¹³ For negative energies, $k^2 < 0$, these representations are infinite dimensional and discrete only if $a_j < -\frac{1}{4}$.¹⁴

In the remainder of this paper we describe group-theoretical properties of the operator \hat{A} , and show how they can be used to obtain quantum numbers for the eigenvalues a_j , and hence for the H^- channel states. These quantum numbers arise naturally in the *zero-order dipole basis*, defined here, in which the matrix of \hat{A}_0 is diagonal. Our use of the zero-order dipole basis as a starting point contrasts with the usual formulation of the dipole representation in terms of the configuration basis.

III. $SO(4)_1 \times SO(4)_2$

A. Hydrogenic basis

The states $|nlm\rangle$ of fixed principal quantum number $n (= 1, 2, \dots)$ are a basis for a finite irreducible representation of an $SO(4)$ algebra^{15,16} generated by the orbital angular momentum \vec{I} and a

vector \vec{b} :

$$\begin{aligned} [l_r, l_s] &= i \mathcal{E}_{rst} l_t, \\ [l_r, b_s] &= i \mathcal{E}_{rst} b_t, \\ [b_r, b_s] &= i \mathcal{E}_{rst} l_t. \end{aligned} \quad (12)$$

Here $r, s, t = 0, 1, 2$ and b_0 is defined by

$$b_0 |nlm\rangle = |n\bar{l}+1m\rangle \left(\frac{(n+l+1)(n-l-1)(l+m+1)(l-m+1)}{(2l+1)(2l+3)} \right)^{1/2} + |nl-1m\rangle \left(\frac{(n+l)(n-l)(l+m)(l-m)}{(2l-1)(2l+1)} \right)^{1/2}. \quad (13)$$

A dynamical representation of \vec{b} is given by the Runge-Lenz operator.¹⁷ It is easily verified that average values of \vec{r} and $\hat{r} (\equiv \vec{r}/r)$ are proportional to \vec{b} within subspaces of constant n ,

$$\vec{r} \rightarrow \frac{3}{2} n \vec{b}, \quad \hat{r} \rightarrow n^{-1} \vec{b}. \quad (14)$$

The $SO(4)$ algebra invariants $b^2 + l^2$ and $\vec{I} \cdot \vec{b}$ have eigenvalues

$$b^2 + l^2 = n^2 - 1, \quad \vec{I} \cdot \vec{b} = 0. \quad (15)$$

B. Representation of \hat{A} with hydrogenic states

The two-electron hydrogenic configuration basis is

$$|Nl, nl'; LM\pi\rangle = \sum_{m, m'} |Nlm\rangle_1 |nl'm'\rangle_2 \langle lm, l'm' | LM \rangle. \quad (16)$$

Within subspaces of constant N and n , \hat{A} has the representation

$$\hat{A} = \hat{l}_2^2 + (3\lambda N/n)(\vec{b}_1 \cdot \vec{b}_2). \quad (17)$$

The key result to be noted here is that in the limit $n \rightarrow \infty$ the matrix of \hat{A} in the hydrogenic configuration basis is identical to that of \hat{A} in the channel-

state configuration basis. This amounts to representing the infinite-dimensional space of angular states $|lm\rangle$, $l=0, 1, \dots$, as the limit of a sequence of finite-dimensional spaces $|nlm\rangle$, $l=0, 1, \dots, n-1$.¹⁸ A physical interpretation of the procedure is that the six-coordinate hydrogenic configuration space reduces effectively to the five-coordinate channel configuration basis upon adiabatically ionizing the outer electron by letting $n \rightarrow \infty$ and hence the average value of r_2 —approach infinity. Thus \hat{A} may be investigated either directly on the channel-state basis or on the hydrogenic configuration basis provided that in the end we let $n \rightarrow \infty$. We choose the latter path since it provides means for direct comparison with previous¹⁻³ doubly-excited-state quantum numbers.

IV. ZERO-ORDER DIPOLE BASIS

A. Configuration-mixed hydrogenic states

For notational convenience we summarize the properties¹⁻³ of the two-electron “doubly excited symmetry basis.” Neglecting exchange the basis is defined for total angular momentum L (we omit the M quantum number) and parity π :

$$|Nn, KTL\pi\rangle = \sum_{l, l'} |Nl, nl'; L\rangle D_{Nl, nl'}^{KTL\pi}, \quad (18)$$

$$D_{Nl, nl'}^{KTL\pi} = (-1)^{l'} [(n+K+T)(n+K-T)(2l+1)(2l'+1)]^{1/2} M_T g_\pi \begin{pmatrix} \frac{1}{2}(N-1) & \frac{1}{2}(n-1) & \frac{1}{2}(n-1+K+T) \\ \frac{1}{2}(N-1) & \frac{1}{2}(n-1) & \frac{1}{2}(n-1+K-T) \\ l & l' & L \end{pmatrix}. \quad (19)$$

K and T are the integer quantum numbers, with allowed values for fixed L :

$$T = 0, 1, \dots, \min(L, N-1)$$

$$K = N-1-T, N-3-T, \dots, -N+3+T, -N+1+T.$$

g_π allows only terms in the summation with $(-1)^{l+l'} = \pi$. M_T is a normalization constant, $M_T = 1$ if $T=0$ and $M_T = 2^{1/2}$ if $T \neq 0$. The quantum numbers

are related to $SO(4) = SO(4)_1 \times SO(4)_2$ algebra invariants as follows:

$$B^2 = (n+K)^2 - 1 + T^2 - L(L+1), \quad (20)$$

$$(\vec{B} \cdot \vec{L})^2 = T^2(n+K)^2, \quad (21)$$

with $\vec{L} = \vec{l}_1 + \vec{l}_2$ and $\vec{B} = \vec{b}_2 - \vec{b}_1$.

From the symmetry properties¹⁹ of the 9- j symbol, we obtain²⁰

$$D_{Nl, n l'}^{K T L \pi} = \pi(-)^{L+T} D_{Nl, n l'}^{K-T L \pi}. \quad (22)$$

Thus only states with $\pi = (-)^L$ can have $T = 0$. We use the convention that $T \geq 0$. Then the complementary set of states having $\pi = (-)^{L+1}$ must have $T \geq 1$.

B. Infinite-dimensional-limit representation

We show now that the zero-order dipole basis (Sec. II C) may be obtained as the infinite- n limit of the hydrogenic basis set. Starting with the representation of $\hat{A}_0 = 2\lambda r_1 \cos\theta_{12}$ in Eq. (17),

$$\begin{aligned} \hat{A}_0 &= (3\lambda N/n)(\vec{b}_1 \cdot \vec{b}_2) \\ &= (3\lambda N/2n)(b_1^2 + b_2^2 - B^2) \\ &= (3\lambda N/2n)(n^2 - B^2 + N^2 - 2 - \hat{l}_1^2 - \hat{l}_2^2). \end{aligned} \quad (23)$$

Substituting the eigenvalues of B^2 from Eq. (20) into the last equation gives

$$\begin{aligned} \hat{A}_0 &= -3\lambda NK + (3\lambda N/2n)[N^2 - 1 - K^2 - T^2 \\ &\quad + L(L+1) - \hat{l}_1^2 - \hat{l}_2^2]. \end{aligned} \quad (24)$$

For fixed N and L the second term vanishes as $n \rightarrow \infty$, and thus

$$\hat{A}_0 = -3\lambda NK, \quad \hat{A}_1 = \hat{l}_2^2. \quad (25)$$

The zero-order dipole basis, denoted $|NKT\pi\rangle$, is derived from a straightforward reduction of Eq. (18) as $n \rightarrow \infty$. The result is

$$|NKT\pi\rangle = \sum_{l, l'} |Nl, l'; LM\rangle C_{ll'}^{KT\pi}, \quad (26)$$

$$\begin{aligned} C_{ll'}^{KT} &= (-)^{\alpha-\alpha'} [(2l+1)(2l'+1)]^{1/2} \\ &\quad \times M_T g_\pi \begin{pmatrix} a & a & l \\ \alpha & \beta & T \end{pmatrix} \begin{pmatrix} l & l' & L \\ T & 0 & -T \end{pmatrix}. \end{aligned} \quad (27)$$

Here we set $a = \frac{1}{2}(N-1)$, $\alpha = -\frac{1}{2}(K+T)$, and $\beta = \frac{1}{2}(K-T)$. Symmetry properties of the 3- j symbols give

$$C_{ll'}^{KT} = (-)^{l+T} C_{ll'}^{-KT}, \quad (28)$$

$$C_{ll'}^{KT} = \pi(-)^{L+T} C_{ll'}^{K-T}, \quad (29)$$

so that when $K=0$ the coefficients vanish unless $l+T$ is even.

C. Representation of \hat{l}_2^2

Matrix elements of $\hat{A}_1 = \hat{l}_2^2$ can be derived in a straightforward manner, and we display here only the final result. \hat{A}_1 does not couple channel states having different values of N . Normalization factors are defined as follows:

$$z_T = (1 + \delta_{T,0})^{1/2}, \quad (30)$$

$$w_T = [1 - \delta_{T,0} + \pi(-)^L \delta_{T,1}]^{1/2}.$$

For notational clarity we drop the labels N , L , and π and use the double notation $|KT(\alpha\beta)\rangle$, where α and β are the equivalent quantum numbers defined following Eq. (27). Then

$$\begin{aligned} A_1 |K, T(\alpha, \beta)\rangle &= |K, T(\alpha, \beta)\rangle [L(L+1) - 2T^2 + 2a(a+1) + 2\alpha\beta] \\ &\quad - |K-2, T(\alpha+1, \beta-1)\rangle [(a-\alpha)(a+\alpha+1)(a+\beta)(a-\beta+1)]^{1/2} \\ &\quad - |K+2, T(\alpha-1, \beta+1)\rangle [(a+\alpha)(a-\alpha+1)(a-\beta)(a+\beta+1)]^{1/2} \\ &\quad + |K+1, T+1(\alpha-1, \beta)\rangle [(L-T)(L+T+1)(a+\alpha)(a-\alpha+1)]^{1/2} z_T \\ &\quad - |K-1, T+1(\alpha, \beta-1)\rangle [(L-T)(L+T+1)(a+\beta)(a-\beta+1)]^{1/2} z_T \\ &\quad - |K+1, T-1(\alpha, \beta+1)\rangle [(L+T)(L-T+1)(a-\beta)(a+\beta+1)]^{1/2} w_T \\ &\quad + |K-1, T-1(\alpha+1, \beta)\rangle [(L+T)(L-T+1)(a-\alpha)(a+\alpha+1)]^{1/2} w_T. \end{aligned} \quad (31)$$

D. Analogy to $SU(3)$ symmetry of strong nuclear interactions

A graphical representation of the allowed values of K and T channels having parity $\pi = (-)^L$ appears in Fig. 1 for thresholds $N=1, 2, 3$, and 4. A similar diagram for channels having $\pi = (-)^{L+1}$ appears in Fig. 2. Each lattice point represents a channel state in the zero-order dipole basis, and is the exact solution to the dipole problem in the non-physical limit of large coupling (i.e., $\lambda \rightarrow \pm\infty$). The allowed values of L for each K, T channel

are $L = T, T+1, T+2, \dots$.

For each N we need consider in what follows only channels having $\pi = (-)^L$. This is valid because there exists an isomorphic mapping from the $N, K, T, L, \pi = (-)^{L+1}$ channels to the $N-1, K, T-1, L-1, \pi = (-)^L$ channels, as comparison of Figs. 1 and 2 readily verifies. For instance, the $N=2, P^e$ channel corresponds to the $N=1, S^e$ channel. In this particular case the channels can support stationary states, $(2p^2)^3P^e$ and $(1s^2)^1S^e$, respectively,²¹ since there are no lower threshold continuum

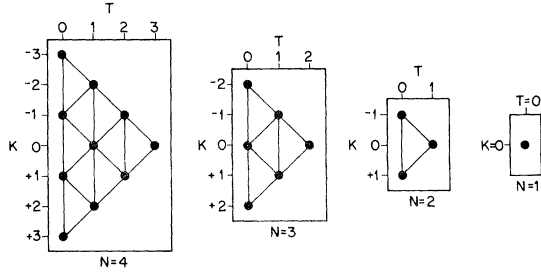


FIG. 1. Values of K and T quantum numbers labeling resonance channels of H^- -like systems having parity $(-)^L$. The lines connecting the channel lattice points represent interactions between channels as specified in Eq. (31).

channels of the same symmetry.

When λ is finite there are interchannel couplings due to \hat{l}_2^2 . These interactions are "weak" for $\lambda > 1$ and low N . They are represented in Figs. 1 and 2 as lines connecting the channel lattice points.

There is an interesting similarity between these representations of the atomic resonance channels and the $SU(3)$ symmetry of strong nuclear interactions. For instance our representation of the $N=4$ channels is identical to that used by Gell-Mann²² to predict the existence²³ of the Ω^- particle in the $\frac{3}{2}^+$ baryon supermultiplet.

This connection is made only for illustrative purposes, and is not intended to suggest a physical relationship between the two problems. Indeed, the electron-hydrogen scattering channels have a different physical origin than the nuclear $SU(3)$. For instance, while our quantum numbers $K/2$ and $-T$ are analogous to the third component of the nuclear isotopic spin and "strangeness," respectively, in labeling each "supermultiplet" of resonance channels, there is in fact no physical connection to be made. A description of the precise origin of the quantum numbers K and T independent of $SO(4)_1 \times SO(4)_2$ appears in Sec. IV E.

E. Physical interpretation of K and T

A conceptual difficulty of the hydrogenic doubly excited symmetry basis is that there is no simple physical interpretation of the quantum numbers

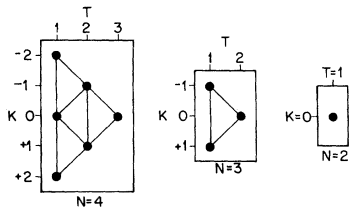


FIG. 2. Values of K and T quantum numbers labeling resonance channels of H^- -like systems having parity $(-)^{L+1}$. (Cf. Fig. 1.)

K and T individually. The inseparability of the quantum numbers is evident in the $SO(4)$ algebra invariants in Eqs. (20) and (21), and results from the coupled motions of the two electrons. This contrasts strongly with the single configuration basis in which the electrons move independently, with l_1 and l_2 diagonal.

In the zero-order dipole basis K and T do have a direct physical interpretation as a result of the uncoupling of the radial motions of the two electrons. From Eq. (25) we see that K is proportional to the average value of $r_1 \cos \theta_{12}$, and thus describes a degenerate Stark-effect mixing with respect to the spatial orientation of the outer electron. The interpretation of T follows upon taking the $n \rightarrow \infty$ limit of Eq. (21), the result being that the square of the matrix of $\vec{L} \cdot \hat{r}_2$ is diagonal, with eigenvalues T^2 . The average motions of \vec{l}_2 and \hat{r}_2 are orthogonal, and thus T describes the magnitude of the overlap $\vec{l}_1 \cdot \hat{r}_2$. Note for fixed N , K , and L that states having the larger values of T will have smaller centrifugal barriers to inward radial motion of the outer electron owing to a concentration of angular momentum in the motion of the inner electron.

Inspection of Eqs. (26) and (27) illustrates the interpretation of K and T as Stark-effect quantum numbers. The states $|NKTL\pi\rangle$ are linear combinations of functions $R_{Nl}(r_1)\Phi(lTL\pi, \hat{\Omega})$, with

$$\Phi(lTL\pi, \hat{\Omega}) = \sum_{l'} \mathcal{Y}(l'l'; L) (2l'+1)^{1/2} \begin{pmatrix} l & l' & L \\ T & 0 & -T \end{pmatrix} \times [1 + \pi(-)^{l+l'}] \frac{M_T}{2}. \quad (32)$$

Here $\hat{\Omega}$ represents the four angular coordinates and $\mathcal{Y}(l'l'; L)$ is a bipolar harmonic. Note that T does not depend on radial coordinates, and from the Wigner-Eckart theorem matrix elements of $\cos \theta_{12}$ between states vanish unless $\Delta l = \pm 1$ and $\Delta T = 0$. This selection rule has importance in the full zero-order basis, where in general $\langle N'K'T'L\pi | r_1 \cos \theta_{12} | NKTL\pi \rangle$ vanishes unless $T' = T$. No similar result holds for K . We emphasize that these interpretations of K and T are valid only in the zero-order dipole basis, but do offer some insight to the understanding of K and T in the hydrogenic basis.

The preceding results indicate clearly the role of $SO(4)$ in the classification of zero-order dipole states. K and T are quantum numbers labeling irreducible representations of a new $SO(4)$ algebra described here. The algebra generators are \vec{I}' and \vec{b}' , defined as the projections of \vec{l}_1 and \vec{b}_1 onto axes of an internal coordinate frame in which \hat{r}_2 is the principal axis. The generators commute with \vec{L} , but $[\pi, (\vec{I}' \cdot \hat{r})] \neq 0$, so that the full rotation-

inversion group must be considered. K and T appear naturally in this description as quantum numbers for the $SU(2) \times SU(2)$ representation of the new $SO(4)$. In addition, matrix elements of \hat{I}_2^2 appearing in Eq. (31) are a direct result of the Wigner-Eckart theorem for $SO(4)$.

V. EIGENVALUES OF \hat{A} AND THE PREDICTION OF H⁻ RESONANCES

A. General properties and perturbation expansion of dipole eigenvalues

In this section we use the notations $A(\lambda)$ and $a(KT\lambda)$ to indicate the λ dependence of the matrix of \hat{A} and its eigenvalues in subspaces of constant N , L , and π . The eigenvalues are even functions of λ about $\lambda = 0$. This follows from a perturbation treatment of $A(\lambda)$ in the configuration basis, where A_1 is diagonal. The configuration states have the one-electron parities, π_1 and π_2 , diagonal. Since A_0 anticommutes with either π_1 or π_2 ,

$$\pi_k A_0 \pi_k = -A_0, \quad (k=1, 2), \quad (33)$$

perturbation coefficients of odd powers of λ vanish. Convergence of the perturbation expansion is assured because for each N, L the channel basis is finite-dimensional.

We offer here a perturbation expansion of the $a(KT\lambda)$ in the zero-order dipole basis—in which A_0 is diagonal—with K and T representing the zero-order quantum numbers. From Eq. (25) it follows that a natural parameter for the expansion is $\eta = (3\lambda N)^{-1}$, with

$$A = -K\eta^{-1} + A_1, \quad (34)$$

$$a(KT\lambda) = \eta^{-1} \sum_{k=0}^{\infty} a_k(KT)\eta^k. \quad (35)$$

The zero-order coefficient is $-K$, so that degenerate perturbation theory must be used to calculate eigenvalues for states having the same K but different T . The zero-order dipole basis is the correct starting point for the degenerate perturbation theory since the interaction matrix A_1 is diagonal in subspaces of constant K .

Using Eq. (33) we see that $A(-\lambda) = \pi_1 A(\lambda) \pi_1$. Thus if $\Phi(KT\lambda)$ is an eigenstate of $A(\lambda)$ having eigenvalue $a(KT\lambda)$ and corresponding to the zero-order state $|NKT\pi\rangle$ at $\lambda = \infty$, then $\pi_1 \Phi(KT\lambda)$ is an eigenstate of $A(-\lambda)$ having the same energy $a(KT\lambda)$. This is a restatement of the fact that the eigenvalues of $A(\lambda)$ are even functions of λ . From Eq. (28) we see that

$$\pi_1 |NKT\pi\rangle = |N - KTL\pi\rangle (-)^T. \quad (36)$$

Thus eigenstates of $A(-\lambda)$ can be obtained in the zero-order basis by letting $K \rightarrow -K$ in the $\Phi(KT)$

states. As a continuous function of λ each zero-order state having K, T quantum numbers at $\lambda = +\infty$ correlates with, and is degenerate with, a zero-order state at $\lambda = -\infty$ having quantum numbers $-K, T$. This implies an “avoided crossing” interaction of the states having $\pm K, T$ symmetrical about $\lambda = 0$. In addition, the expansion coefficients satisfy

$$a_k(-KT) = (-)^{k+1} a_k(KT), \quad (37)$$

so that $a_k(0, T)$ vanishes if k is even.

Using standard formulas²⁴ we have evaluated the perturbation coefficients to second order, the result being

$$\begin{aligned} a(KT\lambda) = & -3N\lambda K + L(L+1) + \frac{1}{2}(N^2 - 1 - K^2 - 3T^2) \\ & - (K/12N\lambda)[8L(L+1) + N^2 - 1 - K^2 - 15T^2] \\ & + O(\lambda^{-2}). \end{aligned} \quad (38)$$

Note that this expression is independent of the total parity. Neglecting higher-order terms, Eq. (38) gives a good estimate of the eigenvalues of \hat{A} in the dipole basis, provided that λ is not too small and N is not too large. Exceptions may occur when $K=0$, owing to the vanishing of terms odd in λ .

B. Comparison with exact $N=2$ results

The $N=2$ resonance channels provide an exactly solvable spectrum for comparison with (38). The eigenvalues of \hat{A} for this threshold have been discussed in a somewhat different form by Seaton.⁴ Using the matrix of A in Eq. (31) we obtain the following:

$$\begin{aligned} a(KT\lambda) = & L(L+1) + 1 - T^2 \\ & - \text{sgn}(\lambda)K[4L(L+1) + 1 + 36\lambda^2]^{1/2}. \end{aligned} \quad (39)$$

There is no λ dependence in the $K=0$ channel, and the same eigenvalue $[=L(L+1)]$ is obtained for both the L^e and L^o states.

A comparison of the exact eigenvalues with the second-order perturbation values appears in Table I for $K=+1$, at $H^-(\lambda=1)$. The agreement is best

TABLE I. Eigenvalues of the dipole operator \hat{A} for $N=2$ resonance channels with $K=+1$, $T=0$. The exact values are from Eq. (39) and the second-order perturbation values from Eq. (38).

L^π	Eigenvalue of \hat{A}	
	Exact	Second-order perturbation theory
S^e	-5.0828	-5.0833
P^o	-3.7082	-3.7500
D^e	-0.8102	-1.0833
F^o	3.7805	2.9167

for $L=0$, but gets worse as L increases. Since $a(+1,0) < -\frac{1}{4}$ only for $L \leq 2$, these are the only channels which can support an infinite number of states. The $K=0$ and $K=-1$ channels have $a(KT) \geq 0$. It is important that second-order contributions to $a(KT\lambda)$ must be included in order to predict correctly the allowed resonance channels. To first order only, the $K=+1$ eigenvalues are $-5, -3, +1$, and $+7$ for $L=0, 1, 2$, and 3 respectively.

C. Comparison with exact dipole eigenvalues for $N=3, 4$

Eigenvalues of $A(\lambda)$ were obtained for $N=3, 4$ by numerical diagonalization. Examples of these results appear in Fig.3 for the $N=3$ D channels ($L=2$) to illustrate features of the λ dependence of eigenvalues described earlier in this section. In general as L increases the parabolic curvature near $\lambda=0$ extends more toward $\lambda=1$, indicating that the second-order perturbation formula will be most accurate at H^- for small L .

The exact and second-order $a(K, T)$ eigenvalues of the H^- resonance dipole channels for $N=3, 4$ appear in Tables II and III, respectively. The perturbation formula gives a good approximation to the eigenvalues and for $N=3$ predicts correctly each of the channels which can support an infinite number of states. For $N=4$ the formula fails to predict the very weakly bound $K=1, T=2, L=3$ channel, and incorrectly predicts a resonance for the $K=3, T=0, L=7$ channel (not shown in Table III). In general, however, the second-order perturbation formula gives good results for the physically important S, P , and D channels, and should be applicable to higher- N thresholds.

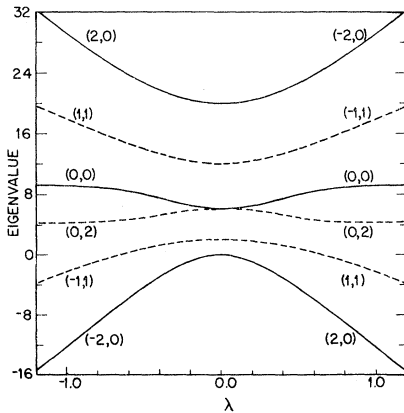


FIG. 3. Eigenvalue spectrum of $\hat{A}(\lambda)$ for the $N=3$ threshold channels having $L=2$. (K, T) denotes the exact zero-order dipole basis quantum numbers in the infinite-coupling limit (i.e., $\lambda = \pm\infty$).

TABLE II. Dipole matrix \hat{A} eigenvalues for $N=3$ H^- channels having $L \leq 4$, parity equal to $(-)^L$. Values (t) from perturbation theory through second order are given for comparison with exact eigenvalues (c).

L	(K, T)					
	(2, 0)	(1, 1)	(0, 2)	(0, 0)	(-1, 1)	(-2, 0)
S c	-16.199	3.951	...	20.248
t	-16.222	4.000	...	20.222
P c	-14.897	-5.220	...	5.602	13.220	23.296
t	-15.111	-5.222	...	6.000	13.222	23.111
D c	-12.249	-2.300	4.365	9.063	17.935	29.186
t	-12.889	-2.111	4.000	10.000	18.111	28.889
F c	-8.171	2.361	10.701	14.503	24.938	37.668
t	-9.556	2.556	10.000	16.000	25.444	37.556
G c	-2.560	8.857	18.974	22.012	34.169	48.548
t	-5.111	8.778	18.000	24.000	35.222	49.111

D. Dipole degeneracies

An interesting feature of the exact eigenvalues $a(KT\lambda)$ is that for fixed N, K, T , and L the eigenvalues are independent of the total parity. Thus the long-range potential describing each channel state having $\pi = (-)^{L+1}$ is degenerate with that of the corresponding K, T channel state having $\pi = (-)^L$. In Tables III and IV the eigenvalues for $\pi = (-)^{L+1}$ are obtained by restricting $T \geq 1$, while all the channels are in the $\pi = (-)^L$ spectrum. To illustrate the difference between the degenerate states, the eigenvector of the $N=3, K=1, T=1, L=1$ channel in the zero-order basis is for *odd parity*

$$-0.257|20\rangle + 1.000|11\rangle - 0.285|00\rangle + 0.065|-11\rangle - 0.028|-20\rangle,$$

while for *even parity* it is

$$1.000|11\rangle + 0.110|-11\rangle.$$

Both channel states have the same eigenvalue, $a(11) = -5.220$, even though the zero-order $|11\rangle$ and $|-11\rangle$ states appear with different relative weights in the even- and odd-parity states.

E. Comparison with experiment and with regularities in calculated spectra

The dipole representation has been used previously for describing long-range properties of the H^- resonance channels.^{4-7,11} However, the new channel quantum numbers K and T provide a means for classifying the resonances to a greater extent. A key result of the present classification is that K and T can be obtained in the infinite-dimensional-limit $SO(4)_1 \times SO(4)_2$ representation of the hydrogen-

TABLE III. Dipole matrix \hat{A} eigenvalues for $N=4$ H^- channels having $L \leq 6$, parity equal to $(-)^L$. Values (t) from perturbation theory through second order are given for comparison with exact eigenvalues (c).

L	(K, T)									
	(3, 0)	(2, 1)	(1, 2)	(1, 0)	(0, 3)	(0, 1)	(-1, 2)	(-1, 0)	(-2, 1)	(-3, 0)
S c	-33.32	-5.34	19.21	...	39.45
t	-33.37	-5.29	19.21	...	39.37
P c	-32.05	-18.46	...	-3.86	...	7.92	...	21.10	30.54	42.81
t	-32.37	-18.50	...	-3.62	...	8.00	...	21.62	30.50	42.37
D c	-29.48	-15.72	-4.84	-0.86	...	11.25	19.49	25.03	35.82	49.31
t	-30.37	-15.83	-5.04	-0.29	...	12.00	19.04	26.29	35.83	48.37
F c	-25.58	-11.53	-0.34	3.77	7.10	16.54	26.62	31.16	43.62	58.65
t	-27.37	-11.83	-0.04	4.71	6.00	18.00	26.04	33.29	43.83	57.37
G c	-20.29	-5.77	6.22	10.12	15.95	23.86	35.88	39.57	53.86	70.60
t	-23.37	-6.50	6.62	11.37	14.00	26.00	35.37	42.62	54.50	69.37
H c	-13.53	1.63	14.77	18.30	26.64	33.27	47.25	50.25	66.44	84.97
t	-18.37	0.17	14.96	19.71	24.00	36.00	47.04	54.29	67.83	84.37
I c	-5.23	10.77	25.28	28.39	39.19	44.77	60.71	63.18	81.29	101.66
t	-12.37	8.17	24.96	29.71	36.00	48.00	61.04	68.29	83.83	102.37

ic configuration basis. This establishes a correspondence between the previous^{1,3} classification of H^- states with the hydrogenic basis set and the present zero-order dipole-basis classification. It was noted in the earlier work that as λ was varied continuously from 0 to 1, only channels having $K > 0$ remained below threshold at H^- . In the present description this selection rule is due primarily to the zero-order dipole operator \hat{A}_0 , originating from $1/r_{12}$, with eigenvalues $\hat{A}_0 \rightarrow -3NK$ at $\lambda = 1$. These zero-order eigenvalues are lower bounds to

the exact eigenvalues of \hat{A} in the dipole representation, since the perturbation $\hat{A}_1 = \hat{l}_2^2$ is positive. Thus it is in general possible only for H^- channels having $K > 0$ to support an infinite number of states below threshold.

The remaining regularities of the H^- resonance spectrum below threshold are described *qualitatively* by the $a(KT)$ expansion to first order;

$$\hat{A} \rightarrow -3NK + L(L+1) + \frac{1}{2}(N^2 - 1 - K^2 - 3T^2). \quad (40)$$

Note for instance that with fixed N , K , and L , the

TABLE IV. H^- resonance channels below the $N=2, 3, 4$ ionization thresholds as predicted in the dipole approximation. K and T are the group-theoretical channel quantum numbers. Resonances actually identified by experiment or theoretical calculation are listed for comparison.

Threshold	Parity	(K, T)	Predicted ^a resonance channels	Identified resonances ^b
$N=2$	$(-)^L$	(1, 0)	S, P, D	$1^3S, 1^3P, 1^1D$
$N=3$	$(-)^L$	(2, 0)	S, P, D, F, G	$1^3S, 1^3P, 1^3D, 1^3F, 1^1G$
	$(-)^L$	(1, 1)	P, D	$1^3P, 3^1D$
	$(-)^{L+1}$	(1, 1)	P, D	$1^3P, 1^3D$
$N=4$	$(-)^L$	(3, 0)	S, P, D, F, G, H, I	$1^3S, 1^3P, 1^3D$
	$(-)^L$	(2, 1)	P, D, F, G	$1^3P, 1^3D$
	$(-)^L$	(1, 2)	D, F	1^3D
	$(-)^L$	(1, 0)	S, P, D	$1^3S, 1^3P, 1^1D$
	$(-)^{L+1}$	(2, 1)	P, D, F, G	$1^3P, 1^3D$
	$(-)^{L+1}$	(1, 2)	D, F	1^3D

^a Using the dipole approximation and exact eigenvalues of \hat{A} .

^b Tabulated data including the K, T classification appears in Refs. 1 and 3. For $N=4$ data are available only for $L \leq 2$.

channels having the larger values of T will be more attractive.

A list of K , T , L channels in which H^- states have been found below the $N=2$, 3, and 4 thresholds appears in Table IV for comparison with the predicted resonance channels in the dipole approximation. Note that the existence of predicted resonances below threshold in the $N=2$ $(1,0)^3D^e$, the $N=3$ $(1,1)^1D^e$, and the $N=4$ $(1,0)^3D^e$ channels has not yet been established.

F. Shape resonances

Although only H^- channels having eigenvalues of \hat{A} less than $-\frac{1}{4}$ can support an infinite number of states, it is possible for the remaining channels to support a finite number of states (usually only one) if the effective nuclear attraction in regions of configuration space where $r_1 \cong r_2$ is large enough. The dominant correlation effect in this region is the angular correlation of nearly degenerate configurations due to $1/r_{12}$. Since the zero-order dipole basis diagonalizes the dipole term in a Legendre expansion of $1/r_{12}$ for large r_1 , we expect that the $K=0$ channel will have the most attractive short-range potential of the H^- channels with $K \leq 0$. This is consistent with the existing¹⁻³ interpretation of hydrogenic configuration mixings.

It is possible for the $K=0$ channels to support states below threshold, as in the case of the $(1s^2)^1S^e$ ground state and the $(2p^2)^3P^e$ doubly excited stationary state. More important, however, is that the present classification scheme verifies the assertion³ that $K=0$ channels are those most likely to support resonances just above threshold, provided that L is not too large. For $N \geq 2$ these states are diffuse, and resonance energies for each N , L , K , T channel will be independent of "short-range" quantum numbers such as exchange and, as we have found in the present paper, parity.

Estimates of possible shape resonance energies have been made³ using linear variational wave functions constructed from a finite hydrogenic basis. This amounts to approximating the $F(l'l', r)$ radial functions in Eq. (2) with a linear combination of hydrogenic radial functions $R_{nl}(r)$, $n=N, N+1, \dots, n_0$. Therefore the calculated energies represent estimates of the shape resonance, as is well known from the stabilization method.²⁵ As $n_0 \rightarrow \infty$, the energies would approach threshold from above.

We reproduce in Table V several of the possible $L=1$ shape resonances to illustrate the insensitivity of the calculated energies to spin and parity differences. The $^1P^o$ resonance at 10.222 eV is well known,⁶ and has been found⁷ to dominate the photoionization cross section just above threshold. This is to be expected upon application of the

TABLE V. Predicted $L=1$ channel H^- shape resonances from Ref. 3, illustrating the insensitivity of the calculated energies to total spin and parity.

Threshold	$^{2S+1}L^\pi$	(K, T)	Energy ^a
$N=2$	$^1P^o$	(0, 1)	10.222
	$^3P^o$	(0, 1)	10.223
$N=3$	$^3P^o$	(0, 1)	12.122
	$^1P^o$	(0, 1)	12.124
$N=4$	$^3P^e$	(0, 1)	12.771
	$^1P^o$	(0, 1)	12.773
	$^1P^e$	(0, 1)	12.787
	$^3P^o$	(0, 1)	12.787

^a In eV above the ground state of H.

$(K, T) = (N-2, 1)$ "selection rule" noted³ for dipole excitation of $\text{He}(\lambda=0.5)$ from the ground state. Extension of the rule to higher H^- threshold predicts in all cases that the strongest excitation channel will lie *below* threshold (i.e., $K > 0$) in contrast to $N=2$ where $K=0$. If indeed this approximate selection rule is applicable in H^- , then the predicted $^1P^o$ shape resonances for $N \geq 3$ should not contribute significantly to the photoionization cross section above threshold.

It is possible that shape resonances associated with the more repulsive $K < 0$ channels may be responsible for unexplained structure in the experimental²⁶ electron impact excitation cross section of H above the $N=2$ and $N=3$ thresholds.

G. Inclusion of exchange and parity effects

The eigenvalues of \hat{A} are essential to the application of energy-level spacing formulas^{5, 6(a), 27-29} for the states within each channel. Numerical values of the energy-level ratio for H^- were reported by Burke.^{6(a)} These formulas cannot, however, predict which channel will support the lowest energy resonance since they do not include exchange effects. Exchange may be handled by using the hydrogenic doubly excited symmetry basis to approximate the configuration mixings when $r_1 \cong r_2$.³ Each Rydberg series of states $n=N, N+1, \dots$, at $\lambda=0$ then correlates with an infinite series of states below threshold in H^- provided that K and L meet the criteria outlined in the preceding sections. Using the properties of the valence states ($n=N$) in the earlier work, we note here²⁰ that the only channels supporting valence states are those with

$$K \geq L - N + 1, \quad (41a)$$

$$\pi(-)^{S+T} = 1. \quad (41b)$$

For example, we see from Table II that the $N=3$ $^1P^o$ channel with $K=2, T=0$ is more attractive than the $K=1, T=1$ channel at long range and we might

expect that the lowest energy state lies in the $K=2$ channel. Inclusion of exchange considerations via (41b) shows, however, that this state is not allowed (by the requirement of antisymmetry), whereas the $K=1$ channel can support a valence state. In fact the lowest-energy $^1P^o$ states of each channel were found³ to lie at 11.92 ($K=1$) and 12.01 eV ($K=2$). As expected from (41b) the situation is reversed for the $N=3$ $^3P^o$ states, with states at 11.76 eV ($K=2$) and 12.07 eV ($K=1$).

In general the energy-level spacing formulas are not applicable to relative positions of valence-type ($n=N$) and excited ($n>N$) states. This explains why the $N=2$ $^1S^e$ and $^3P^o$ series predicted by Temkin and Walker²⁷ tend to be lower in energy than the calculated values.

Condition (41b) for valence states includes explicitly the parity of the channel. Since the H^- states are diffuse, we expect that there may occur near degeneracies between states having the same N , K , T , and L , but different parity and spin. This spin dependence arises because of the different exchange properties of states with $\pi=(-)^L$ and $(-)^{L+1}$. Examples were cited in Table V for predicted shape resonances, but analysis of the calculated³ energies shows that degeneracies also occur for channels below threshold. For instance the $N=3$ $^1P^o$ ($K=1, T=1$) and $^3P^o$ ($K=1, T=1$) states are found at 11.923 and 11.917 eV, respectively. Each state is a valence state, $n=3$. The first excited states ($n=4$) in these channels are also nearly degenerate, occurring at 12.088 and 12.087 eV for odd and even parity, respectively. Similar results are found in other channels for $N=3$ and 4. It appears then that the predicted parity channel degeneracies for eigenvalues of \hat{A} account for these previously unexplained energy degeneracies.

H. Interthreshold couplings

We have neglected the effects of $N \neq N'$ couplings in our classification of resonance channels, primarily because they introduce no essential information to the labeling of the asymptotic region of the channels. We note here that in the zero-order dipole basis, contributions to couplings in the region $r_2 \gg r_1$ due to the dipole term $r_1 \cos \theta_{12}$ of $1/r_{12}$ vanish if the coupling is between states having different values of T (see Sec. IV E). While the present group theory does not provide similar exact selection rules for the full wave function, it is possible to get *approximate* results using physical considerations similar to those employed for He.³ First we note that while K and T were derived here for the long-range interaction, they reflect angular correlations fundamental to the full six-coordinate Hamiltonian, as evidenced by the strong K, T clas-

sifications of H^- states found in the earlier work. Nonradiative decay of the closed-channel resonances to the $(1skL)$ continuum is determined mainly by the properties of the excited state in the region $r_1, r_2 \cong 0$, but autoionization to higher- N threshold continuum channels is more dependent on the relative configuration mixings of the initial and final channels, since both states will have small amplitudes near the nucleus. This effect was noted for He, and should be even more pronounced in H^- . The situation is simplified in H^- since we need consider decay only from the channels with $K>0$.

We expect from our preceding remarks concerning the conservation of T that the strongest transitions between excited threshold channels will be those for which $\Delta T=0$. In addition, the spherical symmetry of $1/r_{12}$ allows that the strongest transitions will be those between states having similar angular and radial correlation of the electrons. We therefore do not expect to see large changes in K for strong decay, so that changes in kinetic energy occur in the relative radial motions of the electrons. A measure of the exchange properties of the states is given by the quantity $\pi(-)^{S+T} \equiv \omega$ in Eq. (41b). The strongest transitions will leave ω unchanged. Since π , L , and S are conserved in Coulomb autoionization this implies that $(-)^T$ is partially conserved. By virtue of footnote 20, this suggests that $(-)^{N+K}$ is also conserved to some degree. Since the strongest interaction is between channels having $\Delta N=-1$, K will change by an odd-integer value.

Together these considerations lead to the following prediction for an approximate selection rule determining the preferred decay channel for an H^- resonance state:

$$(N, K, T, L, \pi, S) \rightarrow (N-1, K \pm 1, T, L, \pi, S), \quad (42)$$

representing the transition from a bound channel state to a continuum channel state. The selection rule is not exact, and breakdowns will most likely occur either through the secondary modes $\Delta T=0$, $\Delta K=\pm 3$ and $\Delta T=1$, $\Delta K=\pm 2$, depending upon the limits of K and T for the thresholds involved, or for $\Delta N=-2$ transitions for which $\Delta T=0$, $\Delta K=0, \pm 2$.

Analysis of the H^- decay modes for $N=3$ to $N=2$ transitions as calculated by Macek and Burke^{6(b)} in the dipole representation shows in fact that the strongest transitions are those in which $\Delta T=0$, $\Delta K=-1$. A more stringent test of our selection rule awaits similar calculations for the $N=4$ resonance decay.

While we stressed that (42) may not be applicable to decay from the $N=2$ closed-channel resonance states it does in fact give the correct result since there is only one possible decay mode, namely,

$N=2, K=1, T=0 \rightarrow N=1, K=0, T=0$ for states with $\pi=(-)^L$. It is also interesting that application of (42) to the $^1P^o$ shape resonance ($N=2, K=0, T=1$) at 10.222 eV predicts a forbidden transition to the $N=1$ channel, suggesting (correctly) that the dominant decay mode is to the $N=2$ continuum channel.

VI. e^+ -H AND p -H RESONANCE CHANNELS

While our primary concern has been the classification of electron-hydrogen compound states, the matrix $A(\lambda)$ appears in other problems where a long-range dipole classification is relevant.²⁹ Most notable are proton-hydrogen ($\lambda=918$) and positron-hydrogen ($\lambda=-1$) scattering. In the latter case the classification of channels may be obtained from the electron-hydrogen results by letting $K \rightarrow -K$. Calculations³⁰ for S^e and P^o channels below the $N=2$ threshold predict a resonance spectrum similar to that of H^- .

The large λ value for proton-hydrogen scattering is due to the relative masses of the electron and proton. A direct consequence of the large λ is that the eigenvalues of $A(\lambda)$ are given to good approximation by the perturbation expansion (38) to first order. Thus

$$a(K, T) = -\frac{3}{2}NKM + L(L+1) + \frac{1}{2}(N^2 - 1 - K^2 - 3T^2) \quad (43)$$

plus corrections of order M^{-1} . Here M is the proton mass in units of the electron mass. With Eq. (43), estimates of the maximum value of the total orbital angular momentum L which support infinite numbers of H_2^+ vibrational states below threshold are easily made. For instance when $K=N-1$ and $T=0$, an infinite number of states can exist in the channel only when $L(L+1) < \frac{3}{2}MN(N-1) - \frac{1}{4}$, owing to the long-range dipole coupling of degenerate electronic and rotational states. Depending on the nature of the short-range interactions, K and T have a potential application in the description of collisional excitation and resonant charge-exchange processes involving these intermediate states of H_2^+ .

From (43) we infer that the adiabatic electronic potential-energy curves of H_2^+ have the asymptotic form

$$E(R) \approx -\frac{1}{2N^2} - \frac{3NK}{2R^2} + O(R^{-3}), \quad (44)$$

where R is the internuclear coordinate. A similar expression was derived by Coulson and Gillam³¹ using the hydrogenic Stark-effect quantum numbers.

Equation (43) can be used also to extend Mittleman's²⁹ zero-order formula predicting vibrational spacings in excited states of H_2^+ , since it includes the first-order rotational corrections.

VII. CONCLUDING REMARKS

We have described a new classification of H^- resonances based on application of group-theoretic techniques to the diagonalization of a strong asymptotic dipole interaction in a close-coupling expansion of the wave function. The method provides two quantum numbers, K and T , which label the resonance channels and lead to accurate predictions of observed resonances using a perturbation expansion of the weaker interactions. Although K and T are related to the K and T quantum numbers found earlier for hydrogenic $SO(4)_1 \times SO(4)_2$ configurations mixings, the present description is in no way a rigorous derivation of the hydrogenic results. This is so because we diagonalize the operator $\vec{b}_1 \cdot \vec{b}_2$, thus providing no information as to which operator, $(\vec{b}_1 - \vec{b}_2)^2$ or $(\vec{b}_1 + \vec{b}_2)^2$, is relevant to the full six-coordinate two-electron problem. While we use $(\vec{b}_1 - \vec{b}_2)^2$ in the present paper $(\vec{b}_1 + \vec{b}_2)^2$ serves equally well, the only difference in the end being the replacement of K with $-K$.

The present method is an improvement over previous dipole-approximation resonance classifications, in which eigenvalues of \hat{A} were simply labeled in increasing order: a_1, a_2, \dots . It also is an improvement over the usual group-theoretic objective of assigning a full set of quantum numbers to each state. Significantly, there exists a classification of the channel states alone, via the factorization in Eq. (2). Subsequent classification of the individual resonance states within each channel would follow from solution of the corresponding radial equations.

ACKNOWLEDGMENTS

I wish to thank Dr. F. H. Stillinger and Dr. J. C. Tully for helpful discussions.

*Present address: Chemistry Department, University of Oregon, Eugene, Oregon 97403.

¹D. R. Herrick, Ph. D. thesis (Yale University, 1973) (unpublished).

²O. Sinanoğlu and D. R. Herrick, *J. Chem. Phys.* **62**,

886 (1975).

³D. R. Herrick and O. Sinanoğlu, *Phys. Rev. A* **11**, 97 (1975).

⁴M. J. Seaton, *Proc. Phys. Soc. Lond.* **77**, 174 (1961).

⁵M. Gailitis and R. Damburg, *Proc. Phys. Soc. Lond.*

- 82, 192 (1963).
- ⁶(a) P. G. Burke, *Adv. Phys.* **14**, 521 (1965); (b) J. Macek and P. G. Burke, *Proc. Phys. Soc. Lond.* **92**, 351 (1967).
- ⁷H. A. Hyman, V. L. Jacobs, and P. G. Burke, *J. Phys.* **B 5**, 2282 (1972).
- ⁸M. Gell-Mann and Y. Ne'eman, *The Eightfold Way* (Benjamin, New York, 1964).
- ⁹G. J. Schulz, *Rev. Mod. Phys.* **45**, 378 (1973).
- ¹⁰E. U. Condon and G. H. Shortley, *The Theory of Atomic Spectra* (Cambridge U. P., Cambridge, England, 1935).
- ¹¹P. G. Burke, *Adv. At. Mol. Phys.* **4**, 173 (1968).
- ¹²L. D. Landau and E. M. Lifshitz, *Quantum Mechanics*, 2nd ed. (Pergamon, New York, 1965), Sec. 35.
- ¹³D. R. Herrick and O. Sinanoğlu, *Phys. Rev. A* **5**, 2309 (1972).
- ¹⁴A. O. Barut and C. Fronsdal, *Proc. R. Soc. Lond.* **287**, 532 (1965).
- ¹⁵V. Fock, *Z. Phys.* **98**, 145 (1935).
- ¹⁶V. Bargmann, *Z. Phys.* **99**, 576 (1936).
- ¹⁷W. Pauli, *Z. Phys.* **33**, 879 (1925).
- ¹⁸This representation is valid only for $l \ll n$, a condition which is satisfied in our application.
- ¹⁹For properties of vector coupling coefficients we have relied upon the compilation of D. M. Brink and G. R. Satchler, *Angular Momentum*, 2nd ed. (Clarendon, Oxford, England, 1968).
- ²⁰Note that $(-)^{N-1-K} = (-)^T$.
- ²¹A more fundamental relationship between these states has been derived. See D. R. Herrick and F. H. Stillinger *Phys. Rev. A* **11**, 42 (1975).
- ²²M. Gell-Mann, *Proceedings of the 1962 International Conference on High-Energy Physics* (CERN Scientific Information Service, Geneva, 1962), p. 805.
- ²³V. Barnes *et al.*, *Phys. Rev. Lett.* **12**, 204 (1964).
- ²⁴See, for example, p. 34 of Ref. 10.
- ²⁵H. S. Taylor, *Adv. Chem. Phys.* **18**, 91 (1970).
- ²⁶J. W. McGowan, J. F. Williams, and E. K. Curley, *Phys. Rev.* **180**, 132 (1969).
- ²⁷A. Temkin and J. F. Walker, *Phys. Rev.* **140**, A1520 (1965).
- ²⁸M. H. Mittleman, *Phys. Rev.* **147**, 73 (1966).
- ²⁹M. H. Mittleman, *Phys. Rev.* **152**, 76 (1966).
- ³⁰G. J. Seiler, R. S. Oberoi, and J. Callaway, *Phys. Rev. A* **3**, 2006 (1971).
- ³¹(a) C. A. Coulson and C. M. Gillam, *Proc. R. Soc. Edinb. A* **62**, 362 (1947); (b) see also D. R. Bates and R. H. G. Reid, *Adv. At. Mol. Phys.* **4**, 13 (1968).